Experimental Test of Sinai's Model in DNA Unzipping

Cathelijne ter Burg, Paolo Rissone, Marc Rico-Pasto, Felix Ritort, Kay Jörg Wiese

Experimental Test of Sinai's Model in DNA Unzipping

Cathelijne ter Burg,[1] Paolo Rissone,[2] Marc Rico-Pasto,[2] Felix Ritort,[2,3] and Kay Jörg Wiese[1]
[1]Laboratoire de Physique de l'Eć ole Normale Supérieure, ENS, Université PSL, CNRS, Sorbonne Université, Université Paris-Diderot, Sorbonne Paris Cité, 24 rue Lhomond, 75005 Paris, France
[2]Small Biosystems Lab, Condensed Matter Physics Department, Universitat de Barcelona, Carrer de Martí i Franquès 1, 08028 Barcelona, Spain
[3]Institut de Nanociència i Nanotecnologia (IN2UB), Universitat de Barcelona, 08028 Barcelona, Spain

(Received 6 October 2022; accepted 4 April 2023; published 16 May 2023)

The experimental measurement of correlation functions and critical exponents in disordered systems is key to testing renormalization group (RG) predictions. We mechanically unzip single DNA hairpins with optical tweezers, an experimental realization of the diffusive motion of a particle in a one-dimensional random force field, known as the *Sinai model*. We measure the unzipping forces F_w as a function of the trap position w in equilibrium and calculate the force-force correlator $\Delta_m(w)$, its amplitude, and correlation length, finding agreement with theoretical predictions. We study the universal scaling properties since the effective trap stiffness m^2 decreases upon unzipping. Fluctuations of the position of the base pair at the unzipping junction u scales as $u \sim m^{-\zeta}$, with a *roughness exponent* $\zeta = 1.34 \pm 0.06$, in agreement with the analytical prediction $\zeta = \frac{4}{3}$. Our study provides a single-molecule test of the functional RG approach for disordered elastic systems in equilibrium.

DOI: 10.1103/PhysRevLett.130.208401

Introduction.—Heterogeneity and disorder pervade physical and biological matter [1–3]. Since Schrödinger's conception of the gene as an a-periodic crystal [4], disorder is recognized as a crucial ingredient for life [5]. The readout of the genetic information encoded in DNA can be modeled with polymers in random potentials, such as Sinai's model [6]. The latter describes the dynamics of a particle diffusing in a one-dimensional random-force field, a suitable model for the mechanical unzipping of the DNA double helix into single strands. Sinai's model is a special case ($d = 0$) of the universal field theory of disordered elastic systems in d dimensions, where one can analytically calculate force correlations. The latter were measured in contact-line depinning ($d = 1$) [7], Barkhausen noise ($d = 2$) [8], and RNA-DNA peeling ($d = 0$) [9]. While these experiments are for depinning, i.e., nonequilibrium, an experimental test of the equilibrium universality class is lacking. Here we test universality of equilibrium-force correlations as predicted by Sinai's model in DNA unzipping. The model parameters are naturally changed during the experiment, allowing us to monitor the functional RG flow.

In the experiment, a DNA hairpin of 6.8 k base pairs (bps) is held between two beads. One is fixed at the tip of a micropipette, the other is optically trapped [Fig. 1(a) and Supplemental Material [10], Sec. A]. By moving the optical trap at a speed $v \approx 10$ nm/s, the double-stranded DNA (dsDNA) is mechanically pulled and converted into two single strands (ssDNA). The measured force-distance curve (FDC) shows a sawtooth pattern characteristic of stick-slip dynamics [Fig. 1(b), red curve]. The hairpin unzips at a critical mean pinning force $f_c \approx 15$ pN, fluctuating in the range 12–17 pN. Once the hairpin is unzipped, the reverse process starts [Fig. 1(b), blue curve]: the optical trap moves backward and the hairpin refolds into the dsDNA native conformation. The absence of hysteresis between rezipping and unzipping FDCs and the fact that there is a single reaction coordinate, implies that the system is in equilibrium.

During unzipping, the base pair at the junction separating dsDNA from ssDNA is subject to random forces generated by the neighboring monomers, and modeled by the motion of a single particle ($d = 0$) in a random potential that belongs to Sinai's universality class [6]. The number of unzipped bps is a well-defined reaction coordinate. Opening (closing) one bp can be seen as a particle hopping to the right (left). We changed salt concentration from 10 mM to 1000 mM NaCl, Fig. 1(c), modulating the strength of bp interactions.

The model.—The motion of the base pair at the junction can be modeled by a Langevin equation (see Supplemental Material [10], Sec. B for the derivation)

$$\frac{\partial u}{\partial t} = m^2(w - u) + F(u) + \eta_u(t), \tag{1}$$

where $u(t)$ is the extension of the molecular construct, w the relative trap-pipette position [Fig. 1(a)], and m^2 the effective stiffness of the molecular construct. The random force is $F(u) = -V'(u)$, where $V(u)$ is the free energy

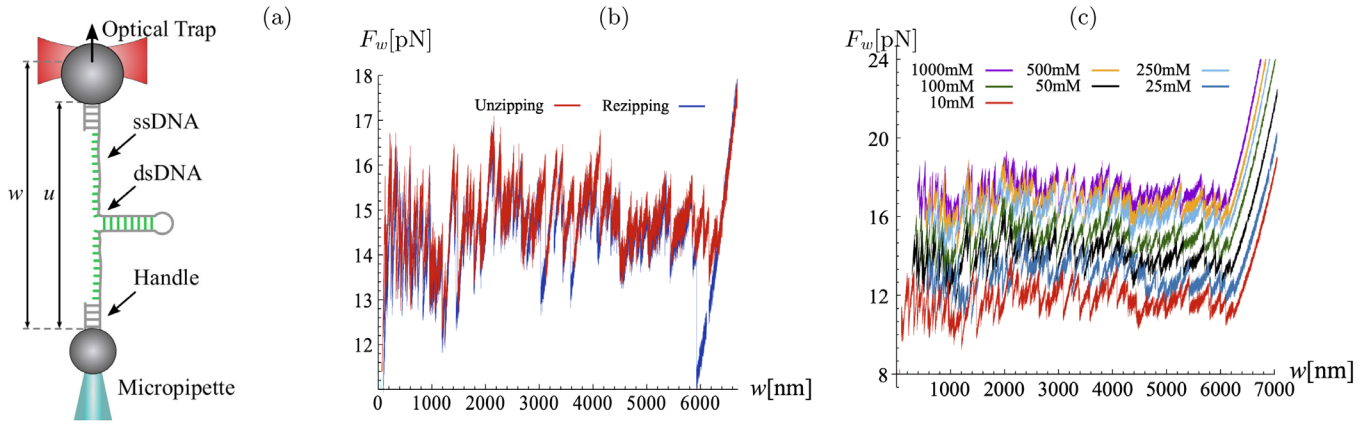

FIG. 1. (a) Experimental setup. (b) Unzipping (red) and rezipping (blue) FDC's demonstrating equilibrium behavior. The residual hysteresis at the end of the FDC is due to the DNA end-loop that slows down the initiation of stem formation upon reconvolution. (c) Experimental FDC's, F_w, for various salt concentrations. The mean pinning force varies between 12–17 pN, and is nonuniversal.

stored in the partially hybridized hairpin. $F(u)$ acts at the hairpin junction and is determined by hydrogen bonding and stacking interactions between consecutive base pairs. Using the nearest-neighbor model one can show that these forces are random, and that their distribution is roughly a Gaussian (Supplemental Material [10], Sec. C). In equilibrium, $(\partial u/\partial t) \approx 0$, so the force $F(u)$ applied to the hairpin in Eq. (1) is counteracted by the force F_w exerted on the bead by the optical trap. For a fixed trap position w, F_w, and u fluctuate due to the thermal noise and the bp breathing dynamics. The equilibrium force correlations are defined as

$$\Delta_{m,T}(w - w') = \overline{F_w F_{w'}}^c = \overline{F_w F_{w'}} - \overline{F_w}\,\overline{F_{w'}}, \qquad (2)$$

where $\overline{(\ldots)}$ stands for a double thermal and disorder average. Correlations depend on the value of m^2, through the m dependence in Eq. (1). They also depend on temperature T, which leads to a rounding of $\Delta_{m,T}(w)$ at small w (see below).

The FDCs in Figs. 1(b) and 1(c) show a sawtooth pattern characterized by segments of increasing force F_w, followed by abrupt drops caused by the cooperative unzipping of groups of base pairs in the range of 10–100 base pairs [13].

The slope of each segment, equivalent to the effective stiffness m^2, decreases with w, permitting us to measure the scaling of $\Delta_{m,T}(w)$ with m^2. In fact, m^2 depends on the combined effects of the optical trap, and the elastic response of the molecular construct (ssDNA and dsDNA handles). It can be written as [see Supp. Mat. Eq. (B27)]

$$\frac{1}{m^2} = \frac{1}{k_b} + \frac{w}{\overline{z_1} k_1}, \qquad (3)$$

with k_b the trap stiffness, and $\overline{z_1}$, k_1 the mean extension and stiffness of one nucleotide at the unzipping force. Modeling the elastic response of the hairpin [14] shows that $k_1 \approx 130$ pN/nm and $\overline{z_1} \approx 0.45$ nm at the unzipping force $f_c \approx 15$ pN, which gives a slope of about $(\overline{z_1} k_1)^{-1} \approx 0.02$ pN^{-1}. Equation (3) implies that the larger the length of the unpaired DNA, the lower the effective stiffness m^2. To verify this, we split the FDCs into four regions (inset of Fig. 2). While smaller regions have smaller variations in m^2, regions must be taken sufficiently large for a reliable statistics. Equation (3) agrees with the experimental data shown in Fig. 2.

Force correlations in Sinai's model can be framed in terms of the functional renormalization group (FRG). The FRG arises as the field theory of disordered systems for interfaces [15–27], generalizing the $d = 0$ case described by the Sinai model. The FRG predicts two universality

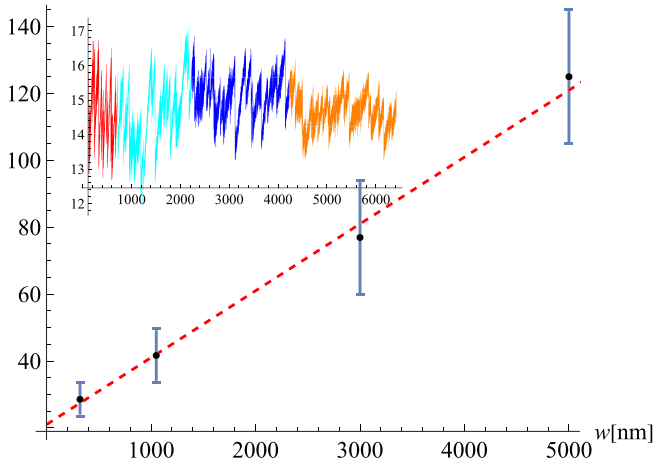

FIG. 2. Variation of the effective stiffness m^2 versus w according to Eq. (3). The points correspond to the measured values of $1/m^2$ for the four FDC regions (each one shown with a different colour in the inset). The fit to data (dashed line) and the extrapolation to $w = 0$ gives the stiffness of the optical trap, $k_b = 0.05 \pm 0.01$ pN $\cdot$ nm^{-1}. The inset illustrates the four studied regions in a FDC at 1M NaCl.

classes, critical depinning (nonequilibrium) and equilibrium (considered here). In equilibrium, the $T \to 0$ limit of $\Delta_{m,T}(w)$ in Eq. (2), can be written as

$$\Delta_m(w) = m^4 \rho_m^2 \tilde{\Delta}(w/\rho_m), \qquad \rho_m \sim m^{-\zeta}, \tag{4}$$

with $\tilde{\Delta}(\mathsf{w})$ the shape function, ζ the roughness exponent, and $\mathsf{w} = w/\rho_m$ the rescaled dimensionless distance. The FRG allows for observables to be computed perturbatively in an expansion around the upper critical dimension, parameterized by $\varepsilon = 4 - d$. The shape function $\tilde{\Delta}(\mathsf{w})$ is the fixed point of the FRG flow equation

$$0 = (\varepsilon - 2\zeta)\tilde{\Delta}(\mathsf{w}) + \zeta \mathsf{w} \tilde{\Delta}'(\mathsf{w}) - \frac{1}{2}\partial_{\mathsf{w}}^2[\tilde{\Delta}(\mathsf{w}) - \tilde{\Delta}(0)]^2 + \ldots \tag{5}$$

The dots represent higher-loop corrections in ε, currently known up to 3-loop order [21–23,25,26,28]. For the equilibrium random field, $\zeta = (4-d)/3$, which gives $\zeta = 4/3$ for $d = 0$. This result is derived by integrating Eq. (5) from $\mathsf{w} = 0$ to $\mathsf{w} = \infty$. It is exact to all orders in the loop expansion. Equation (5) predicts that $\tilde{\Delta}(\mathsf{w})$ has a cusp at $\mathsf{w} = 0$ which is rounded at finite T. Generalization of the FRG equation (5) to finite T allows us to estimate the size of the rounded region. An explicit relation between $\Delta_m(w)$ and $\Delta_{m,T}(w)$ was derived in [15–17],

$$\Delta_{m,T}(w) \approx \mathcal{N} \Delta_m(\sqrt{w^2 + t^2}), \qquad t = \frac{6m^2 k_B T}{\varepsilon |\Delta_m'(0)|}. \tag{6}$$

It has been shown that the RG flow (5) preserves the area under $\Delta_{m,T}(w)$ for all T [28]. Therefore, we can use the measured $\Delta_{m,T}(w)$ and Eq. (6) to determine the normalization factor $\mathcal{N}$ and $\Delta_m(w)$. Details about the procedure are given in Supplemental Material [10], Sec. D.

For the Sinai model, the shape function $\tilde{\Delta}$ in Eq. (5) is known analytically [15,29],

$$\begin{aligned}\tilde{\Delta}(\mathsf{w}) = &-\frac{e^{-\frac{\mathsf{w}^3}{12}}}{4\pi^2\sqrt{\mathsf{w}}} \int_{-\infty}^{\infty} d\lambda_1 \int_{-\infty}^{\infty} d\lambda_2 e^{-\frac{(\lambda_1-\lambda_2)^2}{4\mathsf{w}}} \\ &\times e^{i\frac{\mathsf{w}}{2}(\lambda_1+\lambda_2)} \frac{\mathrm{Ai}'(i\lambda_1)}{\mathrm{Ai}(i\lambda_1)^2} \frac{\mathrm{Ai}'(i\lambda_2)}{\mathrm{Ai}(i\lambda_2)^2} \\ &\times \left[1 + 2\mathsf{w} \frac{\int_0^{\infty} dV e^{\mathsf{w}V} \mathrm{Ai}(i\lambda_1 + V)\mathrm{Ai}(i\lambda_2 + V)}{\mathrm{Ai}(i\lambda_1)\mathrm{Ai}(i\lambda_2)}\right].\end{aligned} \tag{7}$$

Here Ai is the Airy function, and $\zeta = 4/3$ as in FRG.

Data analysis.—We analyzed 33 FDCs obtained by unzipping a 6.8 kBP DNA hairpin in a broad range of salt conditions from 10 to 1000 mM NaCl at $T = 298$ K. As illustrated in Fig. 2, we divided each FDC into four regions measuring the force correlations (2) for each region. Force correlations are equal within the experimental resolution for all salt conditions, as shown in Supplemental Material [10], Fig. 7. Although the effective stiffness of the molecular construct m^2 changes with salt, it changes much less than it does over the different unzipping regions for a fixed salt condition. To enlarge statistics we averaged $\Delta_{m,T}(w)$ over all salts. Results for the first region are shown in Fig. 3 (red line with red strip for error bars).

To recover $\Delta_{m,T}(w)$ in Eq. (6) we must subtract two sources of thermal noise, which are visible as a short-range correlated peak at $w \approx 0$: Brownian fluctuations of the bead; and the breathing dynamics (opening and closing) of the DNA base pairs at the junction. First, bead-noise subtraction reduces the peak's amplitude $\Delta_{m,T}(w = 0)$ from ≈ 0.6 pN^2 (red in main plot of Fig. 3) to ≈ 0.5 pN^2 (magenta line in the inset). Second, we estimated the effect of the breathing dynamics from numerical simulations of Sinai's model [28]. This reduces the peak from ≈ 0.5 to ≈ 0.35 pN^2 with a dip of amplitude ≈ 0.3 pN^2 for $w < 1$ nm (cyan curve in the inset). This dip is also seen in simulations [28]. From $\Delta_{m,T}(w)$ we derive the $T = 0$ force correlations, $\Delta_m(w)$, by plotting the experimental data versus $\sqrt{w^2 + t^2}$, see Eq. (6), with t given there ($T = 298$ K, $\varepsilon = 4$, m^2 from Fig. 2). We initially estimate $\Delta_m'(0)$ by extrapolation of the raw data. This gives $\Delta_m(w)$ for $w > t \approx 7$ nm (black continuous line in Fig. 3). The extrapolated $\Delta_m(w)$ for $w < t$ (dot-dashed region) is obtained by fitting a second-order polynomial (black dot-dashed line in Fig. 3). The whole procedure is iterated until convergence of $\Delta_m(w)$ is reached. As a consistency check we used the $T = 0$ theory prediction $\Delta_m(w)$ together with Eq. (6) to calculate $\Delta_{m,T}(w)$ for all regions, see Supplemental Material [10], Fig. 8.

Force correlations in Eq. (6) are described by three parameters: the correlation length ρ_m in the w direction, the

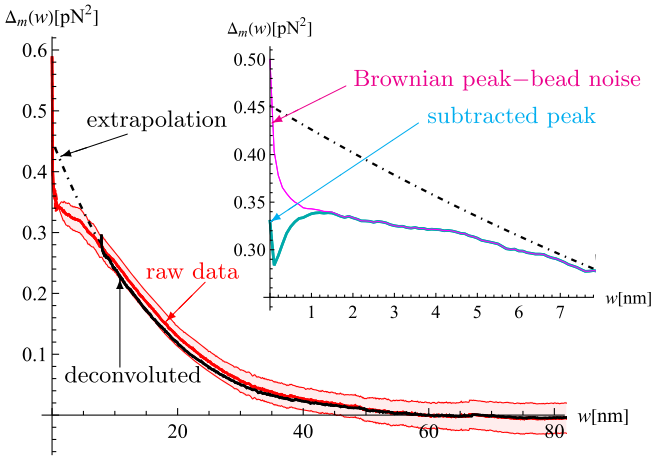

FIG. 3. Measured $\Delta_{m,T}(w)$ for the first region (red). 1σ error is shown as a pink strip. Deconvolution (black solid) and extrapolation to $w = 0$ (black dot-dashed). The inset shows $\Delta_{m,T}(w)$ at short range with subtraction of the peak at $w = 0$, as explained in the main text.

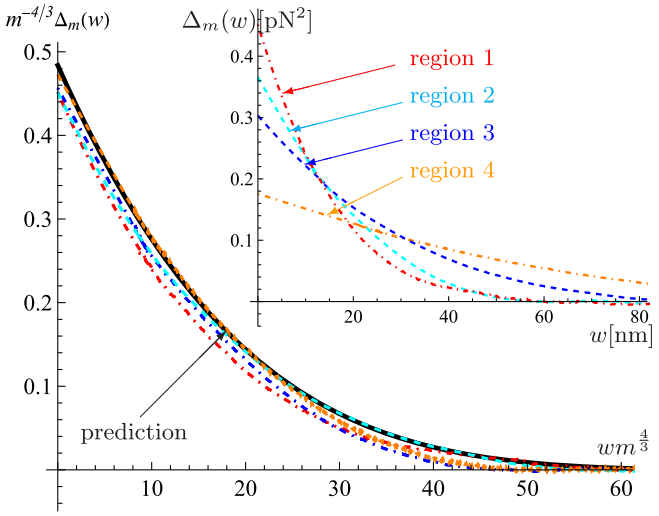

FIG. 4. Inset: The function $\Delta_m(w)$ for the four regions changes with the measured m (see Fig. 5). Main: Collapse of $\Delta_m(w)$ according to Eq. (4) with $\zeta = 4/3$. In black we show the theoretical $\Delta_m(w)$, with $\rho_m = 29(3)$ nm as predicted by the microscopic disorder.

Observable	region 1	region 2	region 3	region 4
w[nm]	[0, 800]	[800,2200]	[2200, 4200]	[4200,6200]
m^2[pN/nm]	0.036(3)	0.027(3)	0.016(4)	0.007(4)
ρ_m [nm]	27(3)	29(3)	42(4)	76(5)
$\Delta_m(0)$[pN^2]	0.44	0.38	0.31	0.18
$\Delta'_m(0)$[pN^2/nm]	0.032	0.018	0.0099	0.0032

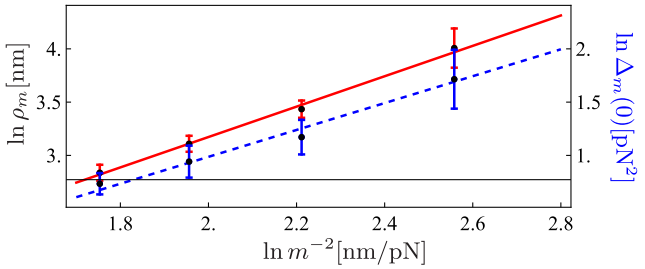

FIG. 5. Top: Properties of the force correlator for the four regions in Fig. 2. The correlation length $\rho_m = C\Delta_m(0)/\Delta'_m(0)$, with $C = \tilde{\Delta}_m(0)/\tilde{\Delta}'_m(0) = 1.36$, see Eq. (7). Bottom: The scaling with m of ρ_m (red, solid), $\zeta = 1.41 \pm 0.10$, and $\Delta_m(0)$ (blue dashed), $\zeta = 1.29 \pm 0.08$. Their mean $\zeta = 1.34 \pm 0.06$ agrees with the expected value, $\zeta = 4/3$.

stiffness m^2 of the molecular construct, and the temperature T. With the measured value of m^2 (Fig. 2) and $k_BT = 4.11$ pN · nm we use Eq. (6) to predict t [$\varepsilon = 4$ and $\Delta'_m(0)$ obtained from the small-w extrapolation in Fig. 3]. According to Eqs. (4) and (6), the scale ρ_m is the only fitting parameter, which we report on the table in Fig. 5 for all four regions. Its value increases with w indicating that FDCs become progressively less rough as unzipping progresses: For the first region, $\rho_m = 26.8$ nm, which corresponds to 33 base pairs [14], the typical size of avalanches that can be resolved in the FDC at the beginning of the unzipping process.

We now check two predictions of the theory: the result (7) and the FRG scaling relation (4). In particular, the scaling function $\tilde{\Delta}$ only depends on the dimensionless combination $w/\rho_m \sim wm^{\zeta}$, and its amplitude is universal. The inset of Fig. 4 shows $\Delta_m(w)$ for the four regions where ρ_m increases while the molecule is unzipped and m^2 decreases. In Fig. 4 we test the scaling law (4) with $\zeta = 4/3$, as predicted for Sinai's model. We can also determine the value of ζ independently of the collapse in Fig. 4. In Fig. 5 we show results for the scaling of the correlation length ρ_m and amplitude $\Delta_m(0)$ with m. We get $\zeta = 1.41 \pm 0.10$ and $\zeta = 1.29 \pm 0.08$ from the scaling of ρ_m and $\Delta_m(0)$, respectively, giving an average of $\zeta = 1.34 \pm 0.06$ in agreement with the expected value $\zeta = 4/3$. Details are given in Supplemental Material [10], Fig. 8.

We can go one step further: In random-field systems, the correlations of the potential $V(u)$ grow linearly at large u distances, $\frac{1}{2}\overline{[V(u) - V(u')]^2} \simeq \sigma|u - u'|$. The constant σ is related to the force correlator Δ_m by

$$\sigma = \int_0^\infty \Delta_\infty(u)du \equiv \int_0^\infty \Delta_m(w)dw. \tag{8}$$

This relation holds for the microscopic $\Delta_\infty(u)$ and the measured $\Delta_m(w)$, as the area under $\Delta_m(w)$ is preserved by the RG flow, as previously discussed. A constant σ in Eq. (8) implies $\zeta = 4/3$ for all m in Eq. (4). Equation (8) then yields the analytic prediction

$$\rho_m = \left[\frac{\int_{w>0}\Delta_\infty(w)}{m^4\int_{w>0}\tilde{\Delta}(w)}\right]^{1/3}. \tag{9}$$

In Supplemental Material [10], Sec. C, we discuss how the microscopic correlator $\Delta_\infty(w)$ can be obtained from the binding energies, using our estimate of $\Delta_\infty(0) \approx 10(2)$ pN^2, which decays to half this value for bp distance 1, and to 0 for bp distance 2, corresponding to 1.6 nm. A linear interpolation of $\Delta_\infty(u)$ between these values gives $\sigma = 8(2)$ pN^2 · nm in Eq. (8). Using $\int_{w>0}\tilde{\Delta}(w) = 0.252$ from Eq. (7), and substituting in Eq. (9) gives $\rho_m = 29(3)$ nm for region 1 in agreement with the value previously obtained ($\rho_m \approx 27$ nm for $m^2 = 0.036$ pN/nm in Fig. 5). In Fig. 4 (main) we show the predicted force correlator (black curve) with the predicted $\rho_m = 29(3)$ nm.

Conclusions.—We tested Sinai's model of equilibrium force correlations and their universality in DNA unzipping experiments. In DNA the binding energies between base pairs are correlated up to two base pairs, making it a suitable realization of Sinai's model. We experimentally measured the roughness exponent ζ finding agreement with Sinai's prediction, $\zeta = 4/3$. While predictions for critical exponents are commonplace, far more difficult is to predict

the amplitude and the correlation length of correlation functions in critical phenomena. Here we show that the amplitude of force correlations and its correlation length can be predicted from the effective stiffness of the molecular construct m^2 and the energy parameters of the nearest-neighbor model in DNA thermodynamics [30,31]. We get experimental values for ρ_m that are within 10% of the predicted ones: e.g., for region 1, $\rho_m \approx 27$ nm (measured) versus $\rho_m \approx 29$ nm (predicted).

It is interesting to compare our unzipping experiment to the peeling of complementary RNA-DNA strands [9]. Peeling is a highly irreversible process belonging to the depinning universality class. It is characterized by a significantly larger effective stiffness m^2, and a larger correlation length of about 186 bp as compared to the 26 to 77 bp of DNA unzipping. The high energies required for DNA peeling make the $T = 0$ nonequilibrium depinning transition relevant there, whereas for DNA unzipping thermal fluctuations occur in equilibrium.

Our study can be extended to DNA with chemically modified bases and RNA [32]. It would also be interesting to study DNA sequences with long-range correlations [33] and with periodically repeated motifs, a physical realization of periodic disorder relevant for charge-density waves. Finally, one could consider dynamical effects, e.g., upon temperature changes [34] using a temperature-jump optical trap [35]. Overall, single-molecule unzipping offers exciting possibilities to experimentally investigate critical phenomena in random polymers.

C. T. B and K. J. W. were supported by LabEx ENS-ICFP. P. R. was supported by the Angelo della Riccia Foundation. M. R.-P. and F. R. were supported by Spanish Research Council Grant No. PID2019–111148 GB-I00 and F. R. by the Instituci Catalana de Recerca i Estudis Avanats, Academia Prize 2018. C. T. B and K. J. W. developed the field theory. F. R. derived the equation of motion from the experimental model. C. T.B analyzed the data. P. R. obtained the experimental data and M. R. set the optical tweezer instrument. All authors contributed to the writing of the Letter.

[1] J.-P. Bouchaud and A. Georges, Anomalous diffusion in disordered media: statistical mechanisms, models and physical applications, Phys. Rep. **195**, 127 (1990).
[2] M. Kardar, Nonequilibrium dynamics of interfaces and lines, Phys. Rep. **301**, 85 (1998).
[3] T. R. Kirkpatrick and D. Thirumalai, Colloquium: Random first order transition theory concepts in biology and physics, Rev. Mod. Phys. **87**, 183 (2015).
[4] E. Schrödinger, *What is Life?* (Cambridge University Press, Cambridge, England, 1992), 10.1017/CBO9781139644129; Nature (London) **171**, 737 (1953).
[5] D. P. Varn and J. P. Crutchfield, What did Erwin mean? The physics of information from the materials genomics of aperiodic crystals and water to molecular information catalysts and life, Phil. Trans. R. Soc. A **374–2063**, 20150067 (2016).
[6] Y. G. Sinai, The limiting behaviour of a one-dimensional random walk in a random environments, Theory Probab. Appl. **27**, 256 (1983).
[7] P. Le Doussal, K. J. Wiese, S. Moulinet, and E. Rolley, Height fluctuations of a contact line: A direct measurement of the renormalized disorder correlator, Europhys. Lett. **87**, 56001 (2009).
[8] C. ter Burg, F. Bohn, F. Durin, R. L. Sommer, and K. J. Wiese, Force-Force Correlations in Disordered Magnets, Phys. Rev. Lett. **129**, 107205 (2022).
[9] K. J. Wiese, M. Bercy, L. Melkonyan, and T. Bizebard, Universal force correlations in an RNA-DNA unzipping experiment, Phys. Rev. Res. **2**, 043385 (2020).
[10] See Supplemental Material at http://link.aps.org/supplemental/10.1103/PhysRevLett.130.208401 for details on the experiment, the effective model, and data analysis. This references [34,35].
[11] J. M. Huguet, C. V. Bizarro, N. Forns, S. B. Smith, C. Bustamante, and F. Ritort, Single-molecule derivation of salt dependent base-pair free energies in DNA, Proc. Natl. Acad. Sci. U.S.A. **107**, 15431 (2010).
[12] J. M. Huguet, M. Ribezzi-Crivellari, C. V. Bizarro, and F. Ritort, Derivation of nearest-neighbor DNA parameters in magnesium from single molecule experiments, Nucl. Acids Res. **45**, 12921 (2017).
[13] J. M. Huguet, N. Forns, and F. Ritort, Statistical Properties of Metastable Intermediates in DNA Unzipping, Phys. Rev. Lett. **103**, 248106 (2009).
[14] A. Alemany and F. Ritort, Determination of the elastic properties of short ssDNA molecules by mechanically folding and unfolding DNA hairpins, Biopolymers **101**, 1193 (2014).
[15] K. J. Wiese, Theory and experiments for disordered elastic manifolds, depinning, avalanches, and sandpiles, Rep. Prog. Phys. **85**, 086502 (2022).
[16] L. Balents and P. Le Doussal, Thermal fluctuations in pinned elastic systems: Field theory of rare events and droplets, Ann. Phys. (N.Y.) **315**, 213 (2005).
[17] P. Chauve, T. Giamarchi, and P. Le Doussal, Creep and depinning in disordered media, Phys. Rev. B **62**, 6241 (2000).
[18] D. S. Fisher, Interface Fluctuations in Disordered Systems: $5 - \varepsilon$ Expansion, Phys. Rev. Lett. **56**, 1964 (1986).
[19] T. Nattermann, S. Stepanow, L.-H. Tang, and H. Leschhorn, Dynamics of interface depinning in a disordered medium, J. Phys. II (France) **2**, 1483 (1992).
[20] O. Narayan and D. S. Fisher, Threshold critical dynamics of driven interfaces in random media, Phys. Rev. B **48**, 7030 (1993).
[21] P. Chauve, P. Le Doussal, and K. J. Wiese, Renormalization of Pinned Elastic Systems: How Does it Work Beyond one Loop?, Phys. Rev. Lett. **86**, 1785 (2001).
[22] P. Le Doussal, K. J. Wiese, and P. Chauve, 2-loop functional renormalization group analysis of the depinning transition, Phys. Rev. B **66**, 174201 (2002).
[23] P. Le Doussal, K. J. Wiese, and P. Chauve, Functional renormalization group and the field theory of disordered elastic systems, Phys. Rev. E **69**, 026112 (2004).

[24] P. Le Doussal, K. J. Wiese, E. Raphael, and R. Golestanian, Can Nonlinear Elasticity Explain Contact-Line Roughness at Depinning?, Phys. Rev. Lett. **96**, 015702 (2006).
[25] K. J. Wiese, C. Husemann, and P. Le Doussal, Field theory of disordered elastic interfaces at 3-loop order: The β-function, Nucl. Phys. **B932**, 540 (2018).
[26] C. Husemann and K. J. Wiese, Field theory of disordered elastic interfaces at 3-loop order: Critical exponents and scaling functions, Nucl. Phys. **B932**, 589 (2018).
[27] R. B. A. Zinati, C. Duclut, S. Mahdisoltani, A. Gambassi, and R. Golestanian, Stochastic dynamics of chemotactic colonies with logistic growth, Europhys. Lett. **136**, 50003 (2022).
[28] C. ter Burg and K. J. Wiese, Force-force correlator for driven disordered systems at finite temperature, arXiv: 2201.12652v1.
[29] P. Le Doussal, The Sinai model in presence of dilute absorbers, J. Stat. Mech. (2009) P07032.
[30] M. Zuker, Mfold web server for nucleic acid folding and hybridization prediction, Nucl. Acids Res. **31**, 3406 (2003).
[31] R. Lorenz, S. H. Bernhart, C. Höner zu Siederdissen, H. Tafer, C. Flamm, P. F. Stadler, and I. L. Hofacker, ViennaRNA package 2.0, Algorithms Mol. Biol. **6**, 26 (2011).
[32] P. Rissone, C. V. Bizarro, and F. Ritort, Stem–loop formation drives RNA folding in mechanical unzipping experiments, Proc. Natl. Acad. Sci. U.S.A. **119**, e2025575119 (2022).
[33] M. Slutsky, M. Kardar, and L. A. Mirny, Diffusion in correlated random potentials, with applications to DNA, Phys. Rev. E **69**, 061903 (2004).
[34] M. Sales, J. P. Bouchaud, and F. Ritort, Temperature shifts in the Sinai model: Static and dynamical effects, J. Phys. A **36**, 665 (2003).
[35] S. De Lorenzo, M. Ribezzi-Crivellari, J. Arias-Gonzalez, S. B. Smith, and F. Ritort, A temperature-jump optical trap for single-molecule manipulation, Biophys. J. **108**, 2854 (2015).